Helium excitation by protons and highly-charged-ion impact

V. D. Rodríguez,[1,*] C. A. Ramírez,[2] R. D. Rivarola,[2] and J. E. Miraglia[3]

[1]*Departamento de Física, FCEyN, Universidad de Buenos Aires, Ciudad Universitaria, 1428 Buenos Aires, Argentina;*
[2]*Instituto de Física de Rosario, Consejo Nacional de Investigaciones Científicas y Técnicas, Universidad Nacional de Rosario,*
Avenida Pellegrini 250, 2000 Rosario, Argentina;
[3]*Instituto de Astronomía y Física del Espacio, Consejo Nacional de Investigaciones Científicas y Técnicas,*
Casilla de Correos 67, Sucursal 28, 1428 Buenos Aires, Argentina

(Received 24 October 1996)

The symmetric eikonal distorted wave method is extended to account for two-electron atom excitation by ion impact. In this formulation (SE2), the interaction between the projectile and each one of the two target electrons is taken into account in the initial and final wave functions by using the eikonal approximation. The active electron notion is not employed as both electrons are treated the same. When single configuration target wave functions are used, the SE2 transition matrix element can be expressed as a convolution of one-electron transition matrix elements. The theory is applied to the study of helium excitation by proton and highly-charged-ion impact. Experimental total and differential cross section data are well reproduced. [S1050-2947(97)06905-9]

PACS number(s): 34.50.Fa

I. INTRODUCTION

The study of hydrogen and helium excitation by ion impact has recently been the object of new interest motivated by the requirement of data for this process for the proper diagnostic of fusion plasma [1,2]. Most of the work on hydrogen excitation by ion impact is theoretical [3–9]. Besides, a good deal of experimental data on helium excitation has been available [10–15] and just a few recent theoretical works are found in the literature [16–25].

This difference may be understood by the fact that a hydrogen target is simpler to treat in a theoretical way than two-electron atoms such as helium. On the other hand, the simplest experimental target is the helium one, because atomic hydrogen is hard to produce in the laboratory. Thus, experiments on helium excitation by multicharged ions [15] have been available earlier than the corresponding ones on hydrogen excitation [26].

One theoretical aspect to be studied in atomic collisions involving two-electron targets is clarifying the role of electron-electron correlation. At present, it is known that the electronic correlation plays a major role when double electron processes are examined [27]. A detailed analysis on the importance of dynamic electron correlation in double electron excitation has been recently done in Ref. [28]. When single-electron processes are considered, the influence of electronic correlations is expected to be feeble [27]. For instance, when comparing the proton-helium excitation cross sections in the first Born approximation with and without correlated target wave functions, their behavior follows the data trend for impact energies larger than 200 keV [16,13]. For lower impact energies or higher projectile charges, the first Born approximation fails as the perturbative regime is

given up. Therefore, as in the one-electron target case, major theoretical efforts have been addressed to improve the projectile-electron interaction description for dealing with atomic electron excitation by ion impact at intermediate energies. Following this line, the restricted Glauber approximation [19] and the Vainshtein-Presnyakov-Sobelman (VPS) approximations [18] have been applied to study He excitation by proton impact. Though no correlated target wave functions were used, those calculations represented a good improvement over the first Born approximation.

Another way to treat the problem is to attempt the solution of the time-dependent Schrödinger equation (TDSE). A good number of close-coupling calculations have been performed for helium excitation by proton impact (for a review see [22]). However, only recently numerical solutions of the TDSE have been addressed to account for the helium excitation by multicharged ion impact [25]. The reason for this lack is that, for highly charged ion impact, the basis set to be employed is considerably increased and the numerical calculations become intractable.

Different distorted wave theoretical methods have been employed to improve both the Glauber and the VPS approximations in the context of hydrogen excitation at intermediate energies [29–31]. One of these methods, the symmetric eikonal [29,30] (SE) has provided a good description of optically allowed transitions on hydrogen by proton and multicharged ions [29,30,32]. Despite its simplicity, this theory has been successfully compared with the sophisticated finite-differences method applied to the solution of the TDSE [7] not only for total cross sections but also for the details of the impact parameter dependent of the excitation probabilities. The SE eikonal theory has been previously employed for the study of heliumlike electron excitation by using the active-electron or one-electron formalism [32–34].

In this work we extend the symmetric eikonal theory for the analysis of two-electron atom excitation considering both

*Electronic address: vladimir@df.uba.ar

electrons in the same manner. In Sec. II, a theory (SE2) is developed by introducing the eikonal wave functions as distorted waves for both the initial and final collision states. Special attention is paid to the proper long distance asymptotic behavior of the wave functions. We also derive an *active-electron* version of the theory (SE2$_{peak}$). This is accomplished by using a peaking approximation of the full SE2 expression and single configuration target wave functions. Results for helium excitation by proton impact and by multicharged ions are presented in Secs. IV and V, respectively. Finally, conclusions are drawn in Sec. VI.

II. THEORY

We are interested in the heliumlike atom excitation by a heavy projectile P (of charge Z_P) impinging with velocity v. The target atom is composed by a nucleus target T (of charge Z_T) and two bound electrons $e_{1,2}$. Atomic units will be used except where indicated. For large projectile M_P and target M_T nuclear masses the system Hamiltonian is given by

$$H = H_T - \frac{1}{2\nu_T} \nabla^2_{\vec{R}_T} - \frac{Z_P}{r_{P_1}} - \frac{Z_P}{r_{P_2}} + \frac{Z_T Z_P}{R}, \quad (1)$$

where H_T is the Hamiltonian of the isolated helium atom

$$H_T = -\frac{1}{2} \nabla^2_{\vec{r}_{T_1}} - \frac{1}{2} \nabla^2_{\vec{r}_{T_2}} - \frac{Z_T}{r_{T_1}} - \frac{Z_T}{r_{T_2}} + \frac{1}{r_{12}}. \quad (2)$$

$\vec{r}_{T_k}$ ($\vec{r}_{P_k}$) are the coordinates of the electron e_k with respect to the target (projectile) nucleus, $\vec{R}$ is the vector position of the projectile with respect to the target nucleus (for large M_T, $\vec{R} \cong \vec{R}_T$), $\nu_T = (M_T + 2m_e)M_P/(M_T + M_P + 2m_e) \cong M_T M_P/(M_T + M_P)$ is the reduced mass, and $\vec{r}_{12} = \vec{r}_{T_1} - \vec{r}_{T_2}$ is the $e_1 - e_2$ coordinate.

The unperturbed Born states are eigenfunctions of Eq. (1) by switching Z_P and they read

$$\Phi_i^B = \psi_i(\vec{r}_{T_1}, \vec{r}_{T_2}) \exp[i\vec{K}_i \cdot \vec{R}_T], \quad (3)$$

$$\Phi_f^B = \psi_f(\vec{r}_{T_1}, \vec{r}_{T_2}) \exp[i\vec{K}_f \cdot \vec{R}_T], \quad (4)$$

where $\psi_j(\vec{r}_{T_1}, \vec{r}_{T_2})$—or $\psi_j(\vec{r}_T)$ for short—describes the electrons of the heliumlike atom in the states j ($j = i, f$) and $\vec{K}_{i(f)}$ is the initial (final) relative momentum.

The incoming and outgoing wave functions should satisfy the long distance asymptotic conditions

$$\Phi_i^{\infty +} = \Phi_i^B E^+[-Z_P(Z_T - 2), \vec{v}; \vec{R}], \quad (5)$$

$$\Phi_f^{\infty -} = \Phi_f^B E^-[-Z_P(Z_T - 2), \vec{v}; \vec{R}], \quad (6)$$

as $R \to \infty$, where the eikonal phases are defined as

$$E^\pm(Z, \vec{v}; \vec{r}) = \exp\left[\mp \frac{Z}{v} \ln(rv \pm \vec{r} \cdot \vec{v})\right]. \quad (7)$$

The differential cross section for the electron excitation $i \to f$ while the projectile is scattered in the solid angle Ω_P is related to the transition matrix element T_{if} by

$$\frac{d\sigma_{if}}{d\Omega_P} = \frac{\nu_T^2}{4\pi^2} |T_{if}|^2. \quad (8)$$

The proper use of Eq. (8) implies that the internuclear interaction is not switched off in the T-matrix calculations. Total cross sections are obtained by integrating on the projectile scattering angles

$$\sigma_{if} = \int d\Omega_P \frac{d\sigma_{if}}{d\Omega_P}. \quad (9)$$

In what follows we obtain the transition matrix element T_{if} in the SE2 theory.

A. Eikonal distorted wave functions

Following the one-electron case, we approximate the collisional wave functions by eikonal distorted waves as

$$\Phi_i^{E2+} = \Phi_i^B d^+(\vec{r}_{P_1})d^+(\vec{r}_{P_2})D^+(\vec{R}_T), \quad (10)$$

$$\Phi_f^{E2-} = \Phi_i^B d^-(\vec{r}_{P_1})d^-(\vec{r}_{P_2})D^-(\vec{R}_T), \quad (11)$$

where the functions $d^\pm$ and $D^\pm$ are expressed in terms of the eikonal phases as follows:

$$d^\pm(\vec{r}) = E^\pm(Z_P, -\vec{v}; \vec{r}), \quad (12)$$

and

$$D^\pm(\vec{R}) = E^\pm(-Z_P Z_T, \vec{v}; \vec{R}). \quad (13)$$

The functions $d^\pm(\vec{r}_{P_1})$ and $d^\pm(\vec{r}_{P_2})$ take into consideration the interaction between the projectile and both electrons and $D^\pm(\vec{R})$ accounts for the internuclear interaction. The eikonal wave functions above are properly normalized and do satisfy the correct long-distance boundary conditions as given by Eqs. (5) and (6), namely $\Phi_j^{E2\pm} \to \Phi_j^{\infty\pm}$ as $R \to \infty$, and $\langle \Phi_j^{E2\pm} | \Phi_{j'}^{E2\pm} \rangle = \delta_{j,j'}$.

B. Electronic wave functions of the heliumlike target

The electronic wave functions $\psi(\vec{r}_{T_1}, \vec{r}_{T_2})$ of the heliumlike atom do not have closed expressions, which is an important difference from the hydrogenic target case. Since we will be dealing single excitation processes, then it is enough to work within the LS orbit-spin coupling [35]. The electronic states are characterized by the total spin S and the total angular momentum L. The ground state has total spin zero, so the orbital wave function must be symmetric. The final orbital wave function is also symmetric since the perturbation in Eq. (1) does not change the total spin. Thus, we are interested in singlet final states.

For simplicity we will restrict ourselves to the use of single configuration wave functions. The initial (ground) state is given by

$$\psi_0(\vec{r}_1, \vec{r}_2) \cong \phi_0(r_1)\phi_0(r_2), \quad (14)$$

and the final (excited) state by

$$\psi_{n^1LM}(\vec{r}_1,\vec{r}_2) \cong (1+\mathcal{P}_{12})\frac{1}{\sqrt{2}} \ \phi_{f_1}(\vec{r}_1)\phi_{f_2}(\vec{r}_2), \quad (15)$$

where the subindices $f_{1,2}$ denote the quantum numbers of the one-electron final orbitals, and $\mathcal{P}_{12}$ is the exchange operator. Single excitation wave functions ψ_{n^1LM} have one of the electrons in the $1s$ state and the other one in the nLM state. The derivation that follows can be easily extended to account for multiconfigurational wave functions.

C. Transition matrix element in the SE2 approximation

The T-matrix element in the distorted wave approximation is obtained by using the eikonal wave functions $\Phi_j^{E2\pm}$. This method represents an extension of the symmetric eikonal SE (or SE1) introduced for one-electron target atoms. The T-matrix element is written as

$$T_{if}^{SE2} = \langle \Phi_f^{E2-}|W_i|\Phi_i^{E2+}\rangle = \langle \Phi_f^{E2-}|W_f^\dagger|\Phi_i^{E2+}\rangle, \quad (16)$$

where $(H-E)\Phi_{i,f}^{E2\pm}=W_{i,f}\Phi_{i,f}^{E2\pm}$, E being the total energy. The residual potentials up to order $1/M_{T,P}$ are given by

$$W_{i,f}=-\sum_{j=1}^{2}\left[\frac{1}{2d^\pm(\vec{r}_{P_j})} \ \nabla_{\vec{r}_{P_j}}^2 d^\pm(\vec{r}_{P_j})\right.$$
$$\left.+\vec{\nabla}_{\vec{r}_{P_j}}\ln d^\pm(\vec{r}_{P_j})\cdot\vec{\nabla}_{\vec{r}_{T_j}}\ln\psi_{i,f}(\vec{r}_T)\right]. \quad (17)$$

Making use of the corresponding wave functions and the residual potentials we obtain

$$T_{if}^{SE2}=\int\int\int d\vec{R}_T d\vec{r}_{T_1}d\vec{r}_{T_2}\exp(i\vec{P}\cdot\vec{R}_T)\rho^{2ia}(1+\mathcal{P}_{12})\rho_2^{-2ia_P}\psi_f^*(\vec{r}_T)d^{-*}(\vec{r}_{P_1})$$

$$\times\left(-\frac{1}{2}\ \nabla_{\vec{r}_{P_1}}^2 d^+(\vec{r}_{P_1})-\vec{\nabla}_{\vec{r}_{P_1}}d^+(\vec{r}_{P_1})\cdot\vec{\nabla}_{\vec{r}_{T_1}}\right)\psi_i(\vec{r}_T), \quad (18)$$

$$\rho=[R^2-(\vec{R}\cdot\hat{v})^2]^{1/2}, \quad \rho_j=[r_{P_j}^2-(\vec{r}_{P_j}\cdot\hat{v})^2]^{1/2}, \quad (19)$$

$a=Z_PZ_T/v$, $a_P=Z_P/v$, and we have neglected an unimportant constant phase factor.

Because of the symmetry of the wave functions $\psi_{i,f}$ with respect to the exchange of the electronic coordinates we can replace $(1+\mathcal{P}_{12})=2$ in Eq. (18). If Eqs. (14) and (15) for the initial and final states of the heliumlike atom are considered, we obtain

$$T_{if}^{SE2}(a)=2\int\int\int d\vec{R}_T d\vec{r}_{T_1}d\vec{r}_{T_2}\exp(i\vec{P}\cdot\vec{R}_T)\rho^{2ia}\rho_2^{-2ia_P}\psi_f^*(\vec{r}_T)\psi_i(\vec{r}_T)d^{-*}(\vec{r}_{P_2})$$

$$\times\left[-\frac{1}{2}\ \nabla_{\vec{r}_{P_1}}^2 d^+(\vec{r}_{P_1})-\vec{\nabla}_{\vec{r}_{P_1}}d^+(\vec{r}_{P_1})\cdot\vec{\nabla}_{\vec{r}_{T_1}}\ln\phi_0(\vec{r}_{T_1})\right], \quad (20)$$

where we explicitly denote the dependence on the internuclear Coulomb parameter a,

$$\psi_f^*(\vec{r}_T)\psi_i(\vec{r}_T)=\frac{1}{\sqrt{2}}\ [\phi_{f_1}^*(\vec{r}_{T_1})\phi_0(\vec{r}_{T_1})\phi_{f_2}^*(\vec{r}_{T_2})\phi_0(\vec{r}_{T_2})+\phi_{f_1}^*(\vec{r}_{T_2})\phi_0(\vec{r}_{T_2})\phi_{f_2}^*(\vec{r}_{T_1})\phi_0(\vec{r}_{T_1})]. \quad (21)$$

For total cross section calculations, we can work with the transition matrix obtained from Eq. (20) by switching off the internuclear interaction ($a=0$). For differential cross sections, we must reintroduce the internuclear interaction through the well-known Coulomb phase (see, for example, [36]).

By introducing the following Fourier transforms,

$$\phi_{f_j}(\vec{r})\phi_0(\vec{r})=\frac{1}{(2\pi)^3}\int d\vec{K}\ \exp(-i\vec{K}\cdot\vec{r})F_{0f_j}(\vec{K}), \quad (22)$$

$$\phi_{f_j}(\vec{r})\vec{\nabla}_{\vec{r}}\phi_0(\vec{r})=\frac{1}{(2\pi)^3}\int d\vec{K}\ \exp(-i\vec{K}\cdot\vec{r})\vec{G}_{0f_j}(\vec{K}), \quad (23)$$

$$B(a;\vec{K})=\frac{1}{(2\pi)^3}\int d\vec{R}\ \exp(-i\vec{K}\cdot\vec{R})\rho^{2ia} \quad (24)$$

$$=\frac{2^{ia}}{\pi K_\perp^{2(1-ia)}}\frac{\Gamma(1-ia)}{\Gamma(ia)}\ \delta(K_z), \quad (25)$$

where $\vec{K}=K_z\hat{v}+\vec{K}_\perp$, Eq. (20) with the internuclear interaction switched off reads

$$T_{if}^{SE2}(0)=\sqrt{2}\int d\vec{K}B(-a_P;\vec{K})(1+\mathcal{P}_{12})F_{0f_1}(\vec{K})T_{0f_2}^{SE1}(0,\vec{K}+P), \qquad (26)$$

with F_{0f_j} being the corresponding form factor. In Eq. (26) $T_{0f_j}^{SE1}$ denotes the one-electron matrix element for the transition from the ϕ_0 orbital to the ϕ_{f_j} one in the SE approximation [30]

$$T_{0f}^{SE1}(a,\vec{Q})=\int\int d\vec{R}_T\,d\vec{r}_{T_1}\,\exp(iQ\cdot\vec{R}_T)\rho^{2ia}\rho_1^{-2ia_P}\phi_f^*(\vec{r}_{T1})\phi_0(\vec{r}_{T1})$$

$$\times\left[-\frac{1}{2d^+(\vec{r}_{P_1})}\,\nabla^2_{\vec{r}_{P_1}}d^+(\vec{r}_{P_1})-\vec{\nabla}_{\vec{r}_{P_1}}\ln d^+(\vec{r}_{P_1})\cdot\vec{\nabla}_{\vec{r}_{T_1}}\ln\phi_0(\vec{r}_{T_1})\right]. \qquad (27)$$

Because of the Dirac delta function, the expression (26) is reduced to a double integral, which must be numerically evaluated.

D. The peaking approximation (SE2$_{peak}$)

It may be observed that the term $B(a;\vec{K})$ in Eq. (25) exhibits a pronounced peak around $K=0$. Thus, we can perform a peaking approximation of the exact SE2 integral expression. To do this, we extract the smooth variation factor $F_{0f_j}(\vec{K})$, evaluated at $\vec{K}=\vec{0}$, from the integral in Eq. (26). The remaining integral in $d\vec{K}$ can be evaluated by expressing the functions $T_{0f_j}^{SE1}(0,\vec{K}+\vec{P})$ and $B(a;\vec{K})$ as integrals on the coordinates to obtain an expression similar to Eq. (20), but with $a=-Z_P/v$ and $Z_P=0$. Again, this phase factor can be switched off for total cross section calculations and reintroduced for differential cross section calculations. Finally, the peaking version of the SE2, SE2$_{peak}$ is given by

$$T_{if}^{SE2_{peak}}(0)=\sqrt{2}(1+\mathcal{P}_{12})F_{0f_1}(\vec{0})T_{0f_2}^{SE1}(0,\vec{P}). \qquad (28)$$

The interpretation of this expression is simple because of its similarity to the Born approximation [16,37]. In fact, the first Born approximation is obtained by replacing the T-matrix elements for one-electron transition in the SE approximation $T_{0f_j}^{SE1}$ by the corresponding ones in the Born approximation $T_{0f_j}^B$. Therefore, the improvement of $T_{if}^{SE2_{peak}}$ with respect to the simple first Born approximation comes from the utilization of $T_{0f_j}^{SE}$ instead of $T_{0f_j}^B$ in Eq. (28). It may be said that the peaking version is a single scattering approximation. The *active* electron is influenced by the projectile through the Coulomb eikonal phase, while the *passive* electron does not account for this interaction, though its influence is considered in the overlaps $F_{0f_j}(\vec{0})$.

III. HELIUM EXCITATION BY PROTON IMPACT

The proton-helium collision is the fundamental system involving two-electron atoms. Therefore, it becomes an important test for any theory working with two-electron atoms. In the present work we study the helium excitation from the ground state to the n^1P excited states. As the helium initial

state we use a wave function obtained by the method of Roothan-Hartree-Fock,

$$\psi_0(r_1,r_2)=\phi_0(r_1)\phi_0(r_2), \qquad (29)$$

where

$$\phi_0(\vec{r})=\sum_{\lambda=1}^5 b_\lambda\varphi_{1s}(Z_\lambda|\vec{r})=\sum_{\lambda=1}^5 b_\lambda\,\frac{Z_\lambda^{3/2}}{\pi^{1/2}}\,\exp(-Z_\lambda r) \qquad (30)$$

with the coefficients b_λ and the charges Z_λ extracted from the Table I by Clementi and Roetti [38]. For the excited states we use

$$\psi_{n^1LM}(\vec{r}_1,\vec{r}_2)=(1+\mathcal{P}_{12})\frac{1}{\sqrt{2}}\,\phi_{nLM}(\vec{r}_1)\varphi_{1s}(2|\vec{r}_2), \qquad (31)$$

where $\varphi_{1s}(Z|\vec{r})$ has the same form as in Eq. (30), and

$$\phi_{nLM}(\vec{r})=N(nL)r^LY_{LM}(\hat{r})\exp[-a(nL)r]$$

$$\times\sum_{k=1}^{n-L}(-1)^{k-1}b(nL,k)r^{k-1} \qquad (32)$$

with the parameters a, b, and N extracted from Table I of Winter and Lin [39]. These parameters were obtained by using the variational principle.

A. Total cross sections

Experimental total cross sections for He excitation by proton impact have been available since 1967 [10]. However, quite recently some sort of inconsistency in the experimental data has been pointed out for proton energies below 100 keV [23]. As a solution, some of the data have been renormalized to the close-coupling theoretical values [23]. Therefore, it is always of interest to produce a new theoretical calculation in order to yield some light on the controversy. In Figs. 1(a) and 1(b) experimental data are shown as well as present theoretical n^1P excitation cross sections. We observe that for proton energies higher than, say, 300 keV, the cross sections calculated with SE2$_{peak}$ and SE2 merge into one with those obtained with the Born approximation. The data by Hippler
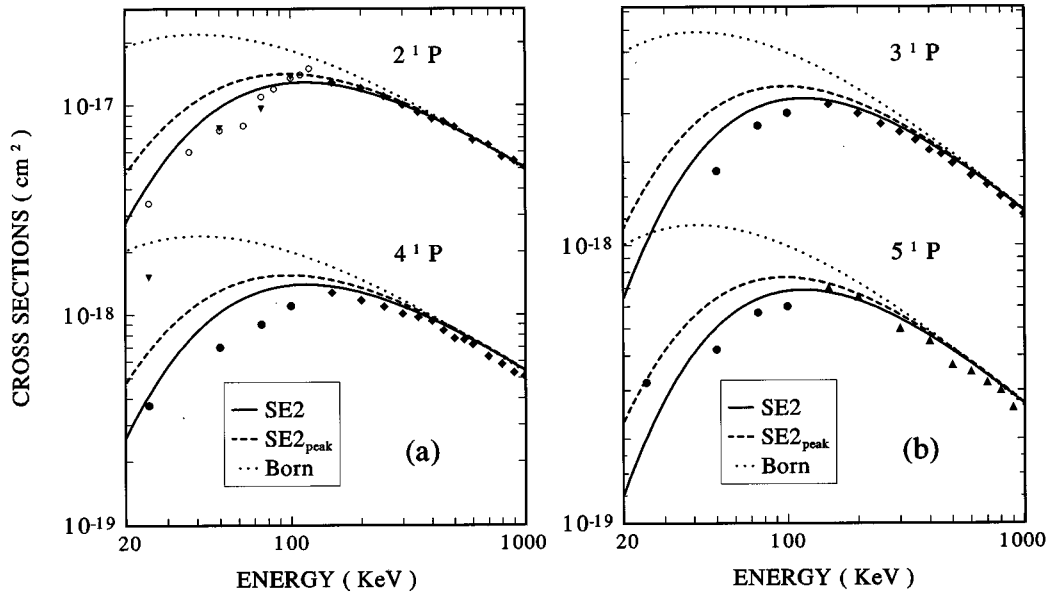
FIG. 1. Total cross section for the excitation of $1\,^1S$ of helium to the $n\,^1P$ states by proton impact. Theory: the solid line, SE2; dashed line, SE2$_{\text{peak}}$; dotted line, first Born approximation. Experiments: Open circles, from Ref. [12]; inverted triangles, from Ref. [14]; diamonds, from Ref. [13]; circles, from Ref. [11]; triangles, from Ref. [10].

and Schartner [13] cover this high-energy range. The agreement between theory and experiment is excellent for $2\,^1P$ and $3\,^1P$ excitations, and differences of the order of 20% can be found for $4\,^1P$. The same can be said for $5\,^1P$ excitation with respect to the van den Bos data [11]. We should recall that differences of this order were found by Bell *et al.* [16] when comparing their first Born approximation with the full correlated wave function with the one obtained using Hartree-Fock wave functions.

For lower energies, the SE2 follows the data trend showing the same experimental qualitative behavior: cross sections decrease for impact energies below 100 keV. This behavior arises from the increasing role of the electron capture channel as the energy decreases. The Born approximation breaks down and overestimates the data by 1 order of magnitude at 20-keV energy. At the lowest energy considered, $E = 20$ keV, the SE2$_{\text{peak}}$ overestimates the SE2 by a factor of 2. The SE2 is clearly much better than the single-active electron version SE2$_{\text{peak}}$ over the whole energy range.

The proton-helium system has been previously studied by using improved versions of the close-coupling approach [23,21,24]. The work by Fritsch is particularly relevant for the low-energy range. With his one-electron close coupling calculations he was able to describe an ondulatory structure in the $1\,^1S$-$N\,^1P$ excitation data between 7 and 40 keV [23]. In Fig. 1 only the $2\,^1P$ excitation cross sections exhibit some structure. The present SE2 just decreases monotonically and is not able to describe this low-energy effect. For the other levels ($N > 2$), the structure is evidenced at lower energies, not shown.

For the $2\,^1P$ excitation case, there is another sophisticated calculation by Grün and co-workers [21]. They have solved the time-dependent Hartree-Fock equations by using a basis set of Gauss-lobe functions. With this basis the matrix elements of the TDHF Hamiltonian can be analytically obtained. Their results for impact energies above 50 keV are in

good agreement with ours as well as with the experimental data. For lower energies, TDHF results show a similar behavior to the SE2 ones; i.e., they overestimate the data without showing any structure.

B. Differential cross sections

Much more sensitive information about the collisional process may be obtained from the differential cross sections. Kvale *et al.* [14] have performed measurements of proton angular differential cross sections for helium excitation at 25-, 50-, 75-, and 100 keV proton impact energies covering the intermediate-energy range.

In Fig. 2, we plot the experimental data along with the present Born, SE, and SE2$_{\text{peak}}$ theoretical calculations. At 25 keV, all these theories fail to follow the data. However, for higher energies the SE2 and SE2$_{\text{peak}}$ are clearly better than the first Born approximation. In particular, the SE2 curve remains within the experimental error bars, and the qualitative agreement with the data is excellent. On the other hand, the SE2$_{\text{peak}}$ agrees with the data to a lower degree than the SE2. First Born results are not good even for 100-keV proton energy. At this energy, the curves are close to each other only in the forward direction. This may be understood by considering that only distant collisions contribute to the forward scattering direction. For distant collisions, the perturbative regime is reached at 100 keV/amu, which is not an impact energy that is too high.

Both the SE2 and SE2$_{\text{peak}}$ differential cross sections show a strong change of the slope around $\theta_{\text{c.m.}} \sim 0.6$–0.7 mrad. This is related to the proper introduction of the internuclear interaction as in the present calculations. Calculations made *without* including the internuclear interaction do not display such a behavior. The experimental data also seem to exhibit this change of slope within the corresponding error bars.

The experimental data were previously compared with theoretical cross sections obtained by using the close-
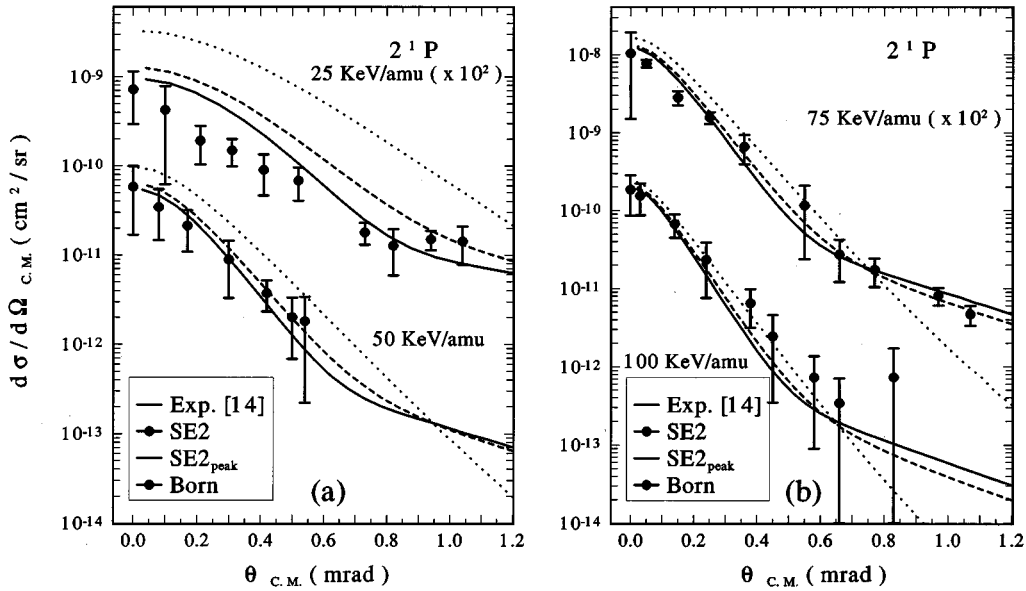
FIG. 2. Angular differential cross section for the excitation of $1\ ^1S$ of helium to $2\ ^1P$ states by 25- to 100-keV proton impact. Curves are denoted as in Fig. 1. Experiments by Kvale *et al.* [14].

coupling method [17], a simplified form of the VPS approximation [18], and the restricted Glauber approximation [19]. Between the two last methods only the Glauber approximation considers both electrons in the same manner. A certain similarity exists between the Glauber theory in the simple scattering approximation [19] and the present $SE2_{peak}$ approximation. In both theories, the two-electron transition matrix element is expressed as products of one-electron transition matrices times orbital overlaps. In the same way the full Glauber approximation [19] is a convolution integral similar to the exact SE2 in Eq. (26).

More recently, Dreizler and co-workers applied an optical-potential description to the study of the proton-helium collision system [24]. They calculated the differential and total cross sections for $2\ ^1P$ helium excitation. They reported differential cross sections for 25- and 100-keV proton impact energies. Their results are in good agreement with the data, and with the present SE2 for 100-keV energy. At 25 keV, their results are in better agreement with the experimental data than present calculations. It is interesting to note that the same change of slope in the differential cross sections can be also observed in the results obtained with this method.

IV. HELIUM EXCITATION BY MUTICHARGED IONS

Most of the theoretical work on atomic excitation by multicharged ion impact done during recent years was devoted to studying the collisions of ions with hydrogen atoms. Just a few theoretical studies are available for helium excitation by highly charged ions [33,3,25]. On the experimental side, Reymann *et al.* [15] reported measurements of helium excitation by multicharged ion impact. The experiments cover a wide range of projectile ion charges, and the impact velocities range from intermediate to high.

From this experimental work, two important features were confirmed. First, the excitation cross sections satisfy the so-called Janev and Presnyakov (JP) scaling rule

$\sigma_{if}/Z_P = f(E/Z_P)$ [40]. Second, the excitation cross sections show apparent saturation as the projectile charge is increased for a fixed impact velocity.

In the next subsections we test in depth the SE2 theory by applying it to the $3\ ^1P$ helium excitation by Si^{6+} ion impact (as a function of the impact energy), and by muticharged ion impact at a fixed velocity (as a function of the projectile charge).

A. Helium excitation by Si^{6+} impact

Experimental total cross sections from Ref. [15] for $3\ ^1P$ He excitation by Si^{6+}, along with SE2, $SE2_{peak}$, and Born theoretical calculations are displayed in Fig. 3 as a function of the projectile impact energy. Different from the case of excitation by proton impact, the Born approximation overestimates the data in the whole specific energy range (up to 1 MeV/amu). It is clear that the perturbative regime is shifted to larger impact energies as the perturbation strength
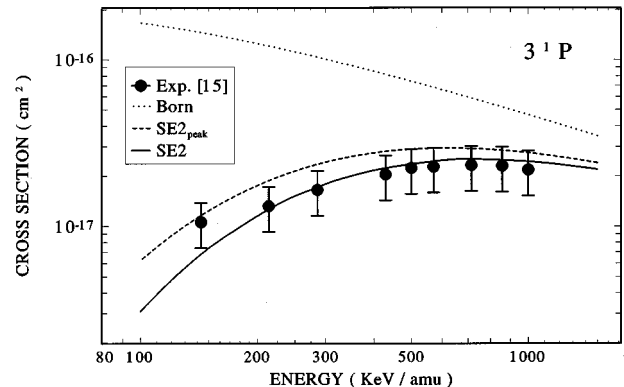
FIG. 3. Total cross section for the excitation of $1\ ^1S$ of helium to the $3\ ^1P$ states by Si^{6+} impact. Curves are denoted as in Fig. 1. Experiments by Reymann *et al.* [15].
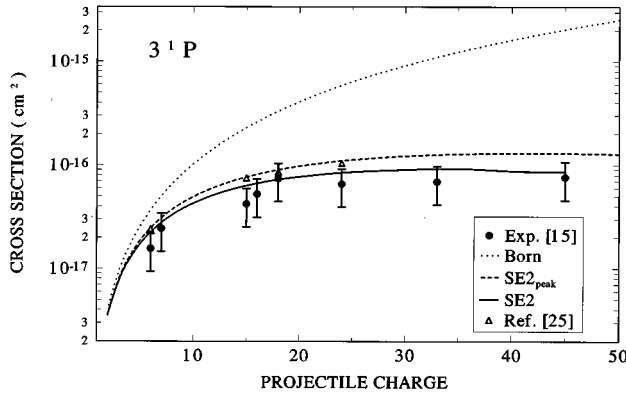
FIG. 4. Total cross section for the excitation of $1\,^1S$ of helium to the $3\,^1P$ states by multicharged ions. Curves are denoted as in Fig. 1. Experiments by Reymann *et al.* [15]. Open triangles are calculations from Ref. [25].

is increased ($Z_P=6$). The exact SE2 explains the data fairly well with the exception of the lowest-energy data (150 keV/amu). The SE2$_{\text{peak}}$ overestimates the SE2, though the differences become smaller as the energy is increased.

The general form of the data can be understood by the JP scaling rule: the basic shape is quite similar to the proton case, provided that the impact energy is properly scaled. Cross sections increase for increasing energies, reach a maximum, and then decrease again for higher energies. The maximum is located around $E/Z_P \sim 100$ keV/amu in a similar way to the proton impact case.

Although not shown here, the SE2 excitation cross sections satisfy the JP scaling rule. This is particularly true for larger projectile charges, as found previously with the SE in the context of hydrogen excitation by multicharged ions [41]. The validity of the JP scaling rule arises from the behavior of the impact-parameter-dependent probabilities. Namely, probabilities show a maximum at a large impact parameter $\rho_M \sim \sqrt{Z_P}$. Therefore, the distant collisions determine the total cross sections and so the dipolar approximation of the interaction potential may be employed. For a dipolar interaction potential, a set of scaling rules including the JP one has been proved to be exact [41].

There exist some calculations for the O^{6+} and C^{6+} impact on He by Fritsch and Lin [42], but these authors only present results for electron capture at impact energies lower than 40 keV/amu.

B. Helium excitation as a function of Z_P

In Fig. 4, excitation cross sections for the same $3\,^1P$ sublevel are shown. Here, the data are plotted for a fixed specific impact energy ($E=1.4$ MeV/amu) as a function of the projectile charge. The data increase as Z_P^2 for low Z_P values, and then increase slowly as Z_P is increased. The theoretical SE2 and SE2$_{\text{peak}}$ curves show a plateau from $Z_P=30$ to $Z_P=40$. For higher projectile charges the cross sections start to decrease very smoothly. The experimental data are accounted for in the SE2 theory within the experimental error bars. The SE2$_{\text{peak}}$ lightly overestimates the SE2 and the experimental data as the projectile charge increases. The improvement of the SE2 over the Born approximation is clearly

appreciated, particularly as the Born cross sections break down for $Z_P > 4$. In the same figure, we show the theoretical results of Martin and Salin [25] obtained with the close-coupling method, which overestimate the data slightly. Unfortunately, no close-coupling results are reported for projectile charges larger than $Z_P=26$ to confirm this trend.

As found by Rodríguez and Salin [7] by solving the TDSE, the apparent saturation of the cross sections may be explained at the level of impact-parameter-dependent probabilities. Namely, the excitation probabilities exhibit a maximum at increasing impact parameters as Z_P is increased. At the same time, the value of this probability maximum decreases with Z_P. As a consequence, total cross sections are similar for a wide range of projectile charges. This later behavior has also been stated by Martin and Salin [25].

The impact-parameter-dependent probabilities evaluated with the present SE2 are in full agreement with the above explanation.

V. CONCLUDING REMARKS

In this work we have presented theoretical calculations of helium excitation to optically allowed levels by proton and multicharged ion impact using the symmetric eikonal theory for two-electron target atoms (SE2). Most of the experimental data are well reproduced for reduced energies E/Z_P larger than 50 keV/amu. An impressive agreement of the full SE2 theory is found for highly charged ion impact, in a similar way to previous applications of the theory with hydrogenic targets. On the contrary, the peaking version of the theory, closely related to an active electron picture, fails to account for the data quantitatively but still exhibits much better performance than the Born approximation.

The theoretical excitation cross sections by multicharged ion impact show a plateau as the projectile charge is increased for a fixed impact velocity. This behavior is known as saturation. However, by extrapolating the present calculations we can say that cross sections start to decrease slowly beyond a finite albeit large value of projectile charge.

Along this work the focus has been on optically allowed transitions $1\,^1S \to N\,^1P$. It is well known that simple distorted waves like the SE describe fairly well these transitions because of their dipolar nature, and because they are basically single-step transitions. No attempt has been made to show results for optically forbidden transitions where second-order refinements are required [31]. More systematic methods such as the close-coupling approximation might be considered better theoretical approaches to deal with these weak transitions.

[1] R. K. Janev, Comments At. Mol. Phys. **26**, 83 (1991).

[2] H. P. Summers, M. von Hellman, F. J. de Heer, and R. Hoekstra, Nucl. Fusion Suppl. **3**, 7 (1992).

[3] R. K. Janev, Phys. Rev. A **53**, 219 (1996).

[4] V. D. Rodríguez and J. E. Miraglia, Phys. Scr. **55**, 455 (1997).

[5] C. A. Ramírez and R. D. Rivarola, Phys. Rev. A **52**, 4972 (1995).

[6] C. A. Ramírez and R. D. Rivarola, J. Phys. B **26**, 3835 (1993).

[7] V. D. Rodríguez and A. Salin, J. Phys. B **25**, L467 (1982).

[8] J. T. Park, Adv. At. Mol. Phys. **19**, 67 (1983).

[9] V. Franco, Phys. Rev. Lett. **20**, 709 (1968).

[10] E. W. Thomas and G. D. Bent, Phys. Rev. **164**, A143 (1967).

[11] J. van den Bos, G. J. Winter, and F. J. de Heer, Physica **40**, 357 (1968).

[12] J. T. Park and F. D. Schowengerdt, Phys. Rev. **185**, A152 (1969).

[13] R. Hippler and K. H. Schartner, J. Phys. B **7**, 618 (1974).

[14] T. J. Kvale, D. G. Seely, D. M. Blankenship, E. Redd, T. J. Gay, M. Kimura, E. Rille, J. L. Peacher, and J. T. Park, Phys. Rev. A **32**, 1369 (1985).

[15] K. Reymann, K. H. Schartner, B. Sommer, and E. Trabert, Phys. Rev. A **38**, 2290 (1988).

[16] K. L. Bell, D. J. Kennedy, and A. K. Kingston, J. Phys. B **1**, 204 (1968).

[17] M. R. Flannery and K. J. MacCann, J. Phys. B **7**, 1558 (1974).

[18] C. E. Theodosiou, Phys. Lett. **83A**, 254 (1981).

[19] S. K. Sur, S. Datta, and S. C. Mukherjee, Phys. Rev. A **24**, 2465 (1981).

[20] M. Kimura and C. D. Lin, Phys. Rev. A **34**, 176 (1986).

[21] K. Gramlich, N. Grün, and W. Scheid, J. Phys. B **19**, 1457 (1986).

[22] W. Fritsch and C. D. Lin, Phys. Rep. **202**, 1 (1991).

[23] W. Fritsch, Phys. Lett. A **160**, 64 (1991).

[24] A. Henne, H. J. Lüdde, and R. M. Dreizler, Z. Phys. D **21**, 307 (1991).

[25] F. Martin and A. Salin, J. Phys. B **28**, 671 (1995).

[26] D. Detleffsen, M. Anton, K. H. Schartner, and A. Werner, J. Phys. B **27**, 4195 (1994).

[27] J. H. McGuire, Adv. At. Mol. Phys. **29**, 17 (1992).

[28] F. Martin and A. Salin, Phys. Rev. A **54**, 3990 (1996).

[29] G. R. Deco, P. D. Fainstein, and R. D. Rivarola, J. Phys. B **19**, 213 (1986).

[30] C. O. Reinhold and J. E. Miraglia, J. Phys. B **20**, 541 (1987).

[31] V. D. Rodríguez and J. E. Miraglia, J. Phys. B **23**, 3629 (1990).

[32] V. D. Rodríguez and J. E. Miraglia, Phys. Rev. A **39**, 6594 (1989).

[33] V. D. Rodríguez and J. E. Miraglia (unpublished).

[34] G. H. Olivera, C. A. Ramirez, and R. D. Rivarola, Phys. Rev. A **47**, 1000 (1993).

[35] H. A. Bethe and E. E. Salpeter, *Quantum Mechanics of One- and Two-Electron Atoms* (Springer, Berlin, 1957).

[36] V. D. Rodríguez, J. Phys. B **29**, 275 (1996).

[37] M. R. C. McDowell and J. P. Coleman, *Introduction to the Theory of Ion-atom Collision* (North-Holland, Amsterdam, 1970).

[38] E. Clementi and C. Roetti, At. Data Nucl. Data Tables **14**, 177 (1974).

[39] T. G. Winter and C. C. Lin, Phys. Rev. A **12**, 434 (1975).

[40] R. K. Janev and L. P. Presnyakov, J. Phys. B **13**, 4233 (1980).

[41] V. D. Rodríguez and J. E. Miraglia, Phys. Lett. A **137**, 123 (1989).

[42] W. Fritsch and C. D. Lin, J. Phys. B **19**, 2683 (1986).